IV Journeys in Multiphase Flows (JEM2017)
March 27-31, 2017 - São Paulo, Brazil

PaperID: JEM-2017-0006

STABILITY SOLVER FOR AIR-WATER HILLY TERRAIN FLOWS

Gabriel Romualdo de Azevedo
gazevedo00@gmail.com
Departamento de Engenharia Mecânica, Escola Politécnica, Universidade de São Paulo, São Paulo, Brazil
Jorge Luis Baliño
jlbalino@usp.br
Departamento de Engenharia Mecânica, Escola Politécnica, Universidade de São Paulo, São Paulo, Brazil
Karl Peter Burr
karl.burr@ufabc.edu.br
Centro de Engenharia, Modelagem e Ciências Sociais Aplicadas, Universidade Federal do ABC, Santo André, Brazil

Abstract. *In risers, the most common flow pattern is intermittent or slug, characterized by an intermittent axial distribution of gas and liquid. This flow pattern may change dramatically under certain geometric and flow conditions leading to an undesirable hydrodynamic instability known as severe slugging. It may have a period of hours, causing higher average pressures, instantaneous flow rates and oscillations at the reservoir. These conditions may lead to the oil production shutdown. Many studies were performed in air-water systems and many stability criteria were developed based on simplified models for vertical risers. Although the stability criteria are useful for a first estimation of the unstable region, a common drawback is that they were not derived from complete dynamic system models, but from ad-hoc conditions in which many physical effects were disregarded; consequently, their applicability is quite limited. As a more efficient alternative to time domain simulations, the linear stability analysis is a powerful technique to identify the stable and unstable regions. In this paper, a stability solver for hilly terrain flow is presented. This solver is an extension of the methodology adopted in the authors' previous works considering a general approach for the void fraction and friction drop through the determination of the local pattern flow*

Keywords: *severe slugging, pipeline-riser system, air-water flow, stability, petroleum production technology*

1. INTRODUCTION

Severe slugging may appear in offshore oil production systems for low gas and liquid flow rates when a section with downward inclination angle (pipeline) is followed by another section with an upward inclination (riser). This phenomenon, characterized by the formation and cyclical production of long liquid slugs and fast gas blowdown, may have a period of hours, causing higher average pressures, instantaneous flow rates and oscillations at the reservoir. These operational conditions may lead to the oil production shutdown. The steps leading to the process of severe slugging formation can be seen in Taitel (1986).

Most of the studies for severe slugging in air-water systems were developed for vertical risers and assume one-dimensional and isothermal flow and a mixture momentum equation in which only the gravitational term is important (Taitel *et al.*, 1990; Sarica and Shoham, 1991). A recent monograph by Mokhatab (2010) reviews different issues related to severe slugging for air-water systems.

In Baliño *et al.* (2010) a model for severe slugging valid for risers with variable inclination was presented. The model was used to simulate numerically the air-water multiphase flow in a catenary riser for the experimental conditions reported in Wordsworth *et al.* (1998). This model was extended for oil-gas-water systems (Nemoto and Baliño, 2012) and for air-water systems including inertial effects and mitigation devices (Baliño, 2012).

Park and Nydal (2014) presented a numerical and experimental study for severe slugging considering a S-shaped riser for an air-water flow. It was adopted a software for flow simulation (OLGA) to compare the results with the experimental data. The results showed a good agreement except for some deviations for slug frequencies at low flow rates. The results regarding the stability maps showed an excellent agreement with the experimental. The experimental data was obtained at the multiphase flow laboratory at the Norwegian University of Science and Technology (NTNU).

Although a pipeline-riser is designed to operate in steady state flow regime, it is possible that this condition does not exist. The stability of a pipeline-riser system depends on the set of parameters defining the operational state. It is common to represent the stability in a map with liquid and gas reference superficial velocities in the axes, leaving the rest of the parameters fixed; then the stability curve is defined as the relationship between the superficial velocities at the stability boundary.

Many stability criteria were developed based on simplified models for vertical risers (Bøe, 1981; Taitel, 1986; Pots *et al.*, 1987; Jansen *et al.*, 1996).

In Bøe (1981) a stability criterion was derived based on the existence of a stratified flow pattern in the pipeline and a

pressure balance at the bottom of the riser, in a condition in which the riser is partially full of liquid only (slug formation stage in a severe slugging type 1 (SS1)). The condition is stated by equalizing the pressure rate in the riser due to the addition of liquid at the bottom and the pressure rate in the pipeline due to the addition of gas. Notice that there are milder severe slugging scenarios such as SS3 (in which there is continuous gas penetration at the bottom of the riser), in which the slug formation stage does not exist.

In Taitel (1986) stability criteria were derived based on the net pressure difference between the riser and the pipeline following the perturbation of a gas pocket penetrating in the riser at the stationary state, considering two boundary conditions: a) constant separation pressure and b) choke valve. Although non-dimensional parameters were obtained with trends in agreement with experimental data, the criteria ignored the flow rate of liquid and gas in the perturbation process. Besides, the non-dimensional parameters depend on variables that are not controlled, such as the void fraction at the pipeline, the mean void fraction at the riser and the void fraction in the gas cap penetrating the liquid column.

Although the stability criteria cited above are useful for a first estimation of the unstable region (they are even used in commercial steady-state computer codes), a common drawback is that they were not derived from complete dynamic system models, but from ad-hoc conditions in which many physical effects were disregarded; consequently, their applicability is quite limited.

The stability curve for any pipeline-riser system can be obtained numerically if a model and a computer simulation program are available. The stationary solution for a given point in the system parameter space is given as initial condition for the numerical simulation; if the numerical solution plus an infinitesimal perturbation (the truncation error in space discretization is enough as a perturbation) converges to the initial condition with time, the stationary solution is stable and it is the system steady state. If the numerical solution goes away with time, the stationary state is unstable, there is no steady state and an intermittent solution develops with time. By changing the point and repeating this process, the stability map can be built. For unstable flow, the analysis of the limit cycle leads to the determination of the flow regime map, showing the regions corresponding to the different types of intermittency.

In Baliño *et al.* (2010), stability and flow regime maps for the multiphase flow in a catenary pipeline-riser system were numerically built. This procedure is laborious and computationally costly, specially for configurations in the parameter space close to the stability boundary, where the time rate of decay or growth of the numerical solution is very small, resulting in very long simulation periods.

As a more efficient alternative to time domain simulations, the linear stability analysis is a powerful technique to identify the stable and unstable regions. To perform the linear stability analysis of a dynamic system we need a model characterized by a set of governing equations. The stationary state is then obtained by setting to zero the time derivatives. Once the stationary state is obtained, the state variables are written as their stationary state value plus a perturbation and are substituted into the governing equations, which gives the perturbation governing equations. Next, these equations are linearized. The linear perturbation governing equations determine how perturbations of the stationary solution evolve with time. The growth rate of the perturbations is given by the real part of the eigenvalues of the spectrum associated with the linearized equations.

In Azevedo *et al.* (2015a), a linear stability analysis was made for the model developed in Baliño *et al.* (2010), considering an arbitrary discretization and including severe slugging mitigation devices such as increase in separation pressure, choke valve at the top of the riser and gas injection at the bottom of the riser. Results were compared with experimental and numerical results reported in the literature with excellent agreement. The results also showed a better agreement with experimental results and with the stability curves obtained through numerical time simulations when the nodalization is increased from the simplest two-node description made in Zakarian (2000).

In Azevedo *et al.* (2015b) it was studied the effect of different void fraction and friction correlation over the stability maps for severe slugging. For the void fraction sensitivity study, results showed that the different correlations give similar stability maps, with very small differences in the near horizontal branch of the stability boundary and slight differences in the near vertical branch. For the friction pressure drop sensitivity study, results showed that it does not affect significantly the stability maps because the mass fluxes are low and the main contribution to the total pressure drop comes from the gravitational term. The different correlations showed the right experimental trend by increasing the unstable region as the equivalent buffer length in the pipeline is increased.

In Azevedo *et al.* (2017) the model presented in Azevedo *et al.* (2015a) is extend to include three different models for the pipeline: a lumped parameters model; a simplified lumped parameters model where the void fraction fluctuation is not neglected; and a third one that considers distributed parameters using the same mathematical approach as the riser. It was compared the three pipeline models seeking to observe the influence of more general modelings over the stability map and differences between these models. It was observed that for higher buffer lengths the models have important differences and the usual void fraction simplification at pipeline is not sufficient to capture the stabilization at the superior branch of stability map. The results show that a simplified model would lose some stable region for operational conditions (superior branch of the stability map), but the complete models would not.

As Bøe (1981), the stabilization of the system is related to the transition from stratified flow to intermittent flow and, numerically, it is possible to capture this effect. The models show the influence of the stratified flow over the stability,

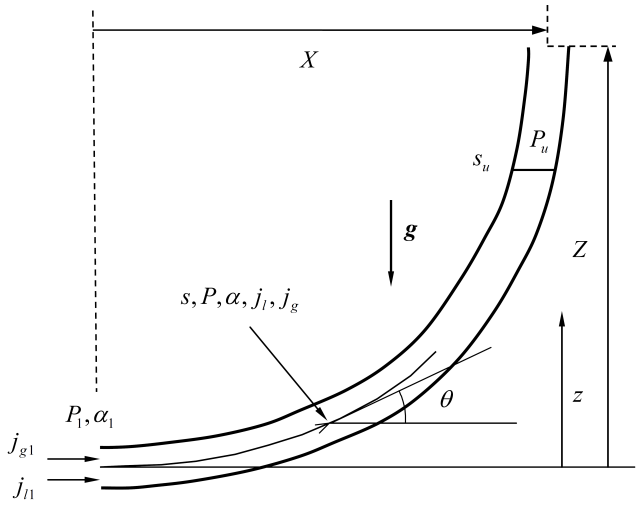

Figure 1. Definition of variables at the riser (from (Baliño, 2012)).

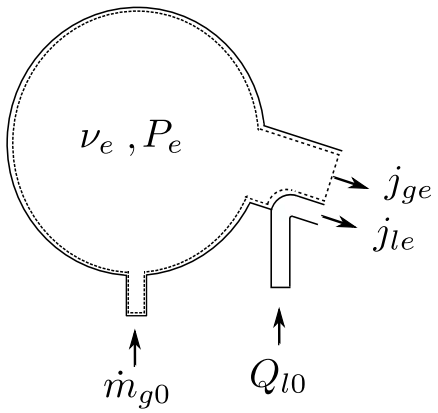

Figure 2. Definition of variables at the buffer volume

however with the simplified lumped model is no possible to observe the effect. The distributed model is expected to give better results. Besides including the void fraction fluctuations, it is more realistic than the lumped models. It allows the propagation of density waves and variations of the state variables with position over the pipeline. The results from Azevedo *et al.* (2017) shows that a more general modeling is necessary to capture all the influence of the stratified flow over stability and over the pipeline dynamics.

For offshore oil production systems, a tool to evaluate the effectiveness of methodologies to suppress or mitigate severe slugging should be of great importance. Linear stability analysis of an adequate model can be used to predict the effectiveness of mitigation/supression methodologies in the resulting stability maps The present work extends the model presented in Azevedo *et al.* (2015a) by including a general model for a air-water hilly terrain flow, including the determination of flow pattern for each riser position and the two-phase multiplier approach to calculate the frictional and gravitational pressure drop. The results are compared to Park and Nydal (2014) and they show an excellent agreement with the experimental data.

Regarding the organization of this paper, Section 2. presents the extended model used for two-phase flow in pipeline-riser systems with; this model allows general geometries with upward and downward inclination. Section 4. presents the stationary state, used as a base solution to obtain the linear perturbation governing equations. Section 5. presents the linear perturbation governing equations for the continuous dynamic system. Section 6. presents the discretized perturbation equations and the determination of the eigenvalues spectrum for the resulting dynamic system with finite number of degrees of freedom. Section 7. shows different results obtained for operating conditions taken from literature, corresponding to experiments in S-shape risers. Finally, Section 8. presents the conclusions.

2. MODEL

Based on Fig. 1, the following equations can be written:

$$-\frac{\partial \alpha}{\partial t} + \frac{\partial j_l}{\partial s} = 0 \tag{1}$$

$$\frac{\partial}{\partial t}(P\,\alpha) + \frac{\partial}{\partial s}(P\,j_g) = 0 \tag{2}$$

A mixture momentum equation is considered, where the inertial terms are neglected:

$$\frac{\partial P}{\partial s} + \rho_m\, g\, \sin\theta + \phi_{f0}^2\, \frac{1}{2}\, f_l\, \frac{G^2}{\rho_l\, D} = 0 \tag{3}$$

where g is the gravity acceleration constant, j_g and j_l are respectively the gas, liquid superficial velocities, P is the pressure, s is the position along the riser, α is the void fraction, ϕ is the two-phase multiplier, μ_l is the liquid dynamic viscosities and ρ_l and ρ_m are respectively the liquid and mixture density and G is the total mass flux. Also, the following relations ca be written:

$$\rho_m = \rho_l\,(1-\alpha) + \frac{P}{R_g\, T_g}\,\alpha \tag{4}$$

$$f_l = f\left(Re_l,\ \frac{\epsilon}{D}\right) \tag{5}$$

$$Re_l = \frac{GD}{\mu_l} \tag{6}$$

And,

$$G = \rho_g j_g + \rho_l j_l \tag{7}$$

In order to calculate the friction pressure gradient term in Eq. (3), the two-phase multiplier ϕ_{f0}^2 is used. According to its definition, the actual friction pressure gradient for the mixture can be obtained as the product of the two-phase multiplier and the friction pressure gradient considering the total mass flowing as liquid phase. It will be assumed that the two-phase multiplier depends algebraically on the local variables as follows:

$$\phi_{f0}^2 = \phi_{f0}^2\left(j_g,\ j_l,\ P,\ \theta\right) \tag{8}$$

The Darcy friction factor f_l depends on the Reynolds number Re_l and the relative roughness ϵ/D, (where ϵ is the pipe roughness) and is calculated from Chen (1979) using a homogeneous mixture two-phase model.

It will be assumed that there is an algebraic relation between the void fraction and the local flow conditions:

$$\alpha = \alpha\left(j_g,\ j_l,\ P,\ \theta\right) \tag{9}$$

As there is an algebraic relation between void fraction and the rest of the variables, given by Eq. (9), the void fraction can be eliminated, decreasing the system order. After some algebra, the dynamic equations (1) to (3) can be written as:

$$\{A\left(\{v\}\right)\} + \underline{B}\left\{\frac{\partial v}{\partial t}\right\} + \underline{C}\left\{\frac{\partial v}{\partial s}\right\} = 0 \tag{10}$$

where:

$$\{v\} = \left\{\begin{array}{c} j_g \\ j_l \\ P \end{array}\right\} \tag{11}$$

$$\{A\} = \left\{\begin{array}{c} 0 \\ 0 \\ A_3 \end{array}\right\} \tag{12}$$

$$A_3 = \rho_m\, g\, \sin\theta + \phi_{f0}^2\, \frac{1}{2}\, f_l\, \frac{G^2}{\rho_l\, D} \tag{13}$$

$$\underline{B} = \left\{\begin{array}{ccc} B_{11} & B_{12} & B_{13} \\ 0 & 0 & B_{23} \\ 0 & 0 & 0 \end{array}\right\} \tag{14}$$

$$B_{11} = -\frac{\partial \alpha}{\partial j_g} \tag{15}$$

$$B_{12} = -\frac{\partial \alpha}{\partial j_l} \tag{16}$$

$$B_{13} = -\frac{\partial \alpha}{\partial P} \tag{17}$$

$$B_{23} = \alpha \tag{18}$$

$$\underline{C} = \left\{\begin{array}{ccc} 0 & C_{12} & 0 \\ C_{21} & C_{22} & C_{23} \\ 0 & 0 & C_{33} \end{array}\right\} \tag{19}$$

$$C_{12} = 1 \tag{20}$$

$$C_{21} = C_{22} = P \tag{21}$$

$$C_{23} = j_g \tag{22}$$

$$C_{33} = 1 \tag{23}$$

2.1 Buffer volume

The existence of a buffer vessel with volume υ_e is considered in order to simulate an equivalent pipeline length $L_e = \frac{\upsilon_e}{A}$, where A is the flow passage area ($A = \frac{1}{4}\,\pi\,D^2$, where D is the inner diameter).

$$Q_{l0} = j_{le}\,A \tag{24}$$

$$L_e \frac{dP_e}{dt} = P_e\,j_{ge} - \frac{T_g}{T_0}\,P_0\,j_{g0} \tag{25}$$

where j_{lb} and j_{gb} are, respectively, the superficial velocities for the liquid and gas at the base of the riser, P_b and P_g are, respectively, the pressure at the base of the riser and the gas pressure, T_g is the gas temperature and t is time

The superficial velocities at a reference condition for gas and liquid, respectively j_{g0} and j_{l0}, used to represent the stability maps, are defined as:

$$j_{g0} = \frac{R_g\,T_0\,\dot{m}_{g0}}{P_0\,A} \tag{26}$$

$$j_{l0} = \frac{Q_{l0}}{A} \tag{27}$$

where $\dot{m}_{g0}$ is the gas mass flow rate injected in the pipeline, R_g is the gas constant and Q_{l0} is the liquid volumetric flow injected in the pipeline. The reference condition is defined for pressure $P_0 = 1.013\,bara$ and temperature $T_0 = 293\,K$.

3. Closure laws

Shoahm (2006) proposes a model, based on properties of the flow and the local inclination, where it is possible to predict the pattern flow for any inclination angle. This approach is adopted in our work to include the transition between patterns.

In typical laboratory facilities for air-water flow, conditions such low gas and liquid mass flux and low pressures are predominant. For these conditions, it is possible to affirm that the flow pattern associated to upward inclination and downward inclination flows are intermittent and stratified, respectively. Shoahm (2006) also gives these patterns and it confirms this assumption.

In order to close de system and to solve the differential equations system, it is necessary to choose specific closure laws. In our work, the flow pattern is defined, then the model sets which friction and void fraction correlation it would adopt, as closure laws, according to the predict pattern.

In our case, it is important to obtain a transition boundary because severe slugging does not occurs for non-stratified flows (Bøe (1981), Almeida and Gonçalves (1999) and Azevedo *et al.* (2017)). For downward inclinations the transition can occurs and it would avoid severe slugging.

According to Shoahm (2006), the mechanism of wave growth is used for the prediction of transition. A finite wave is assumed to exist on the gas-liquid interface of an equilibrium stratified flow. Extending the Kelvin-Helmholtz theory to analyze the stability of finite waves in pipes, Taitel and Dukler (1976) claimed that when the pressure suction force is greater than the gravity force, waves tend to grow and the stratified flow can not be preserved. The analysis leads to the following criterion:

$$u_g > \left(1 - \frac{h_l}{D}\right)\left[\frac{(\rho_l - \rho_g)\;g\;\cos\theta A_g}{\rho_g \frac{dA_l}{dh_l}}\right]^{0.5} \tag{28}$$

where h_L is the liquid hold-up, A_l is the cross sectional area of liquid and θ is the local inclination.

3.1 Non-stratified flow

For non-stratified flow it is adopted the Chexal *et al.* (1992) correlation for the drift flux model and the Müller-Steinhagen and Heck (1986) correlation for the two-phase multiplier. It is assumed a intermittent flow.

3.2 Stratified flow

Based on Taitel and Dukler (1976) approach, it can be written the following momentum equation for the two phases:

$$-A_l\,\frac{dP}{ds} - \tau_{wl}\,S_l + \tau_i\,S_i - \rho_l\,A_l\,g\sin\theta = 0 \tag{29}$$

$$-A_g\,\frac{dP}{ds} - \tau_{wg}\,S_g - \tau_i\,S_i - \rho_g\,A_g\,g\sin\theta = 0 \tag{30}$$

where P is the pressure, s is the position along the flow, τ_{wg} , τ_{wl} e τ_i are the shear stress, respectively, between the gas-wall, liquid-wall and the gas-liquid interface. S_g, S_l e S_i are, respectively, the gas wetted, liquid wetted and gas-liquid interface perimeters.

3.2.1 Void fraction

Combining Eq. (29) and (30) in other to eliminate the total pressure drop, it is obtained:

$$\frac{\tau_{wg} S_g}{\alpha} - \frac{\tau_{wl} S_l}{1-\alpha} + \tau_i S_i \left(\frac{1}{\alpha} + \frac{1}{1-\alpha} \right) + (\rho_l - \rho_g)\, A g \sin\theta = 0 \tag{31}$$

The void fraction for the stratified flow can be estimated by solving the implicit Eq. (31).

3.2.2 Frictional pressure drop

From the combination between Eq. (29) and (30), it can be written:

$$\left. \frac{dP}{ds} \right|_{Friction} = \frac{\tau_{wg} S_g}{A} + \frac{\tau_{wl} S_l}{A} \tag{32}$$

3.3 Continuity between the subsystems

Assuming the same flow passage area for the pipeline and riser, the pressure and superficial velocities at the bottom of the riser are continuous:

$$P(0,t) = P_1(t) = P_e(t) \tag{33}$$

$$j_l(0,t) = j_{l1}(t) = j_{le}(t) \tag{34}$$

$$j_g(0,t) = j_{g1}(t) = j_{ge}(t) \tag{35}$$

Pressure at the top of the riser (position s_t) satisfies:

$$P(s_t,t) = P_s \tag{36}$$

4. STATIONARY STATE

The stationary state, when stable, is the steady state flow operational regime. It is used as the initial condition for the transient simulations and also as the base solution for the linear stability analysis. The stationary state can be obtained by setting to zero the time derivatives in the system governing equations. Variables at stationary state are denoted with superscript $\tilde{}$. The stationary state exists only for the state where there is no $x = 0$ in the pipeline and $s_u = s_t$ in the riser.

Equations (1) and (2) coupling with the buffer modeling Eq. (26) and (27), give:

$$\tilde{j}_l = j_{l0} \tag{37}$$

$$\tilde{j}_g = \frac{T_g}{T_0} \frac{P_0}{\tilde{P}} j_{g0} \tag{38}$$

The void fraction and two-phase multiplier can be calculated from Eq. (8) and (9) as:

$$\tilde{\alpha} = \tilde{\alpha} \left(\tilde{j}_g,\ \tilde{j}_l,\ \tilde{P},\ \theta \right) \tag{39}$$

$$\tilde{\phi} = \tilde{\phi} \left(\tilde{j}_g,\ \tilde{j}_l,\ \tilde{P},\ \theta \right) \tag{40}$$

The pressure distribution can be calculated by numerically integrating Eq. (3), as all terms are functions of pressure and the inclination angle is a function of position; the stationary pressure satisfies:

$$\frac{\partial \tilde{P}}{\partial s} = -\tilde{\rho}_m\, g\, \sin\theta - \tilde{\phi}^2\, \frac{1}{2} \frac{\tilde{f}_l\, \tilde{G}^2}{\rho_l\, D} \tag{41}$$

5. PERTURBATION EQUATIONS

The next step in the linear stability analysis is to linearize the two-phase flow governing equations with respect to a stationary state. As in the previous Section, variables involved in the riser dynamics are written in terms of a stationary state plus a perturbation:

$$j_g = \tilde{j}_g\,(s) + \hat{j}_g\,(s,\,t) \tag{42}$$

$$j_l = \tilde{j}_l\,(s) + \hat{j}_l\,(s,\,t) \tag{43}$$

$$P = \tilde{P}\,(s) + \hat{P}\,(s,\,t) \tag{44}$$

As there is an algebraic relation between void fraction and the rest of the variables, given by Eq. (9), the void fraction is eliminated, decreasing the system order. After some algebra, differential equations for the vector of perturbations of the state variables are finally obtained as:

$$\underline{\tilde{A}}\,\{\hat{v}\} + \underline{\tilde{B}}\left\{\frac{\partial \hat{v}}{\partial t}\right\} + \underline{\tilde{C}}\left\{\frac{\partial \hat{v}}{\partial s}\right\} = 0 \tag{45}$$

where:

$$\hat{v} = \left\{ \begin{array}{c} \hat{j}_g \\ \hat{j}_l \\ \hat{P} \end{array} \right\} \tag{46}$$

$$\underline{\tilde{A}} = \left\{ \begin{array}{ccc} 0 & 0 & 0 \\ \tilde{A}_{21} & 0 & \tilde{A}_{23} \\ \tilde{A}_{31} & \tilde{A}_{32} & \tilde{A}_{33} \end{array} \right\} \tag{47}$$

$$\tilde{A}_{21} = \frac{\partial \tilde{P}}{\partial s} \tag{48}$$

$$\tilde{A}_{23} = \frac{\partial \tilde{j}_g}{\partial s} \tag{49}$$

$$\tilde{A}_{31} = g\,\sin\theta\,\frac{\partial \tilde{\rho}_m}{\partial \tilde{j}_g} + \frac{1}{2\,\rho_l\,D}\,\frac{\partial}{\partial \tilde{j}_g}\left(\tilde{\phi}_{f0}^2\,\tilde{f}_l\,\tilde{G}^2\right) \tag{50}$$

$$\tilde{A}_{32} = g\,\sin\theta\,\frac{\partial \tilde{\rho}_m}{\partial \tilde{j}_l} + \frac{1}{2\,\rho_l\,D}\,\frac{\partial}{\partial \tilde{j}_l}\left(\tilde{\phi}_{f0}^2\,\tilde{f}_l\,\tilde{G}^2\right) \tag{51}$$

$$\tilde{A}_{33} = g\,\sin\theta\,\frac{\partial \tilde{\rho}_m}{\partial \tilde{P}} + \frac{1}{2\,\rho_l\,D}\,\frac{\partial}{\partial \tilde{P}}\left(\tilde{\phi}_{f0}^2\,\tilde{f}_l\,\tilde{G}^2\right) \tag{52}$$

$$\underline{\tilde{B}} = \left\{ \begin{array}{ccc} \tilde{B}_{11} & \tilde{B}_{12} & \tilde{B}_{13} \\ 0 & 0 & \tilde{B}_{23} \\ 0 & 0 & 0 \end{array} \right\} \tag{53}$$

$$\tilde{B}_{11} = -\frac{\partial \tilde{\alpha}}{\partial \tilde{j}_g} \tag{54}$$

$$\tilde{B}_{12} = -\frac{\partial \tilde{\alpha}}{\partial \tilde{j}_l} \tag{55}$$

$$\tilde{B}_{13} = -\frac{\partial \tilde{\alpha}}{\partial \tilde{P}} \tag{56}$$

$$\tilde{B}_{23} = \tilde{\alpha} \tag{57}$$

$$\underline{\tilde{C}} = \left\{ \begin{array}{ccc} 0 & \tilde{C}_{12} & 0 \\ \tilde{C}_{21} & \tilde{C}_{22} & \tilde{C}_{23} \\ 0 & 0 & \tilde{C}_{33} \end{array} \right\} \tag{58}$$

$$\tilde{C}_{12} = \tilde{C}_{33} = 1 \tag{59}$$

$$\tilde{C}_{21} = \tilde{C}_{22} = \tilde{P} \tag{60}$$

$$\tilde{C}_{23} = \tilde{j}_g \tag{61}$$

6. DISCRETIZED PERTURBATION EQUATIONS AND STABILITY ANALYSIS

6.1 Discretized perturbation equations

Each riser interval length is discretized in N_t nodes and Eq. (45) is integrated in the interval $s_i \leq s \leq s_{i+1}$. The total number of nodes at this problems is $N = N_t \times N_i$, where N_i is the number os intervals. In this approach, we have two types of nodes. Those where the properties are continuous and those where the inclination angle has a discontinuity, between two intervals. In the second situation, continuity conditions are written for the state variables. Representative values for any function ϕ within the integration interval are:

$$\phi\left(\tilde{v}\right) = \phi_{i+1/2} \simeq \tfrac{1}{2}\left[\phi\left(\tilde{v}_i\right) + \phi\left(\tilde{v}_{i+1}\right)\right] \quad \text{for} \quad s_i \leq s \leq s_{i+1} \tag{62}$$

The space and time derivatives are calculated as:

$$\left(\tfrac{\partial \hat{v}}{\partial s}\right) = \left(\tfrac{\partial \hat{v}}{\partial s}\right)_{i+1/2} \simeq \tfrac{\hat{v}_{i+1} - \hat{v}_i}{\Delta s_i} \quad \text{for} \quad s_i \leq s \leq s_{i+1} \tag{63}$$

$$\left(\tfrac{\partial \hat{v}}{\partial t}\right) = \left(\tfrac{\partial \hat{v}}{\partial t}\right)_{i+1/2} \simeq \tfrac{1}{2}\left(\tfrac{d\hat{v}_i}{dt} + \tfrac{d\hat{v}_{i+1}}{dt}\right) \quad \text{for} \quad s_i \leq s \leq s_{i+1} \tag{64}$$

where $\Delta s_i = s_{i+1} - s_i$. The following set of equations is obtained:

$$\underline{G}\left\{\frac{d\underline{\hat{v}}}{dt}\right\} + \underline{H}\left\{\underline{\hat{v}}\right\} = 0 \tag{65}$$

$$\underline{G} = \begin{bmatrix} \underline{G_{11}} & \underline{G_{12}} & \underline{G_{13}} \\ \underline{0} & \underline{0} & \underline{G_{23}} \\ \underline{0} & \underline{0} & \underline{0} \end{bmatrix} \tag{66}$$

$$\underline{H} = \begin{bmatrix} \underline{0} & \underline{H_{12}} & \underline{0} \\ \underline{H_{21}} & \underline{H_{22}} & \underline{H_{23}} \\ \underline{H_{31}} & \underline{H_{32}} & \underline{H_{33}} \end{bmatrix} \tag{67}$$

In Eq. (65), $\underline{G}$ and $\underline{H}$ are rectangular sparse matrices with dimension $[3 \times N_i \times (N_t - 1)] \times 3\,N$, while $\underline{\hat{v}}$ is the vector with the nodal values of the perturbed variables ($3\,N$ components) defined as:

$$\left\{\underline{\hat{v}}\right\}_j = \begin{cases} \hat{j}_{g\,j} & \text{for} \quad 1 \leq j \leq N \\ \hat{j}_{l\,j-N} & \text{for} \quad N+1 \leq j \leq 2\,N \\ \hat{P}_{j-2N} & \text{for} \quad 2\,N+1 \leq j \leq 3\,N \end{cases} \tag{68}$$

The sub-matrices defined in Eq. (66) and (67) are rectangular matrices with dimension $(N_t - 1) \times N$, with the following non-zero elements:

$$\left\{G_{11}\right\}_{i,\,i} = \left\{G_{11}\right\}_{i,\,i+1} = \frac{1}{2}\left\{\tilde{B}_{11}\right\}_{i+1/2} \tag{69}$$

$$\left\{G_{12}\right\}_{i,\,i} = \left\{G_{12}\right\}_{i,\,i+1} = \frac{1}{2}\left\{\tilde{B}_{12}\right\}_{i+1/2} \tag{70}$$

$$\left\{G_{13}\right\}_{i,\,i} = \left\{G_{13}\right\}_{i,\,i+1} = \frac{1}{2}\left\{\tilde{B}_{13}\right\}_{i+1/2} \tag{71}$$

$$\left\{G_{23}\right\}_{i,\,i} = \left\{G_{23}\right\}_{i,\,i+1} = \frac{1}{2}\left\{\tilde{B}_{23}\right\}_{i+1/2} \tag{72}$$

$$\left\{H_{12}\right\}_{i,\,i} = -\left\{H_{12}\right\}_{i,\,i+1} = -\frac{\left\{\tilde{C}_{12}\right\}_{i+1/2}}{\Delta s_i} \tag{73}$$

$$\left\{H_{21}\right\}_{i,\,i} = \frac{1}{2}\left\{\tilde{A}_{21}\right\}_{i+1/2} - \frac{\left\{\tilde{C}_{21}\right\}_{i+1/2}}{\Delta s_i} \tag{74}$$

$$\{H_{21}\}_{i,\,i+1} = \frac{1}{2}\left\{\tilde{A}_{21}\right\}_{i+1/2} + \frac{\left\{\tilde{C}_{21}\right\}_{i+1/2}}{\Delta s_i} \tag{75}$$

$$\{H_{22}\}_{i,\,i} = -\{H_{22}\}_{i,\,i+1} = \frac{\left\{\tilde{C}_{22}\right\}_{i+1/2}}{\Delta s_i} \tag{76}$$

$$\{H_{23}\}_{i,\,i} = \frac{1}{2}\left\{\tilde{A}_{23}\right\}_{i+1/2} - \frac{\left\{\tilde{C}_{23}\right\}_{i+1/2}}{\Delta s_i} \tag{77}$$

$$\{H_{23}\}_{i,\,i+1} = \frac{1}{2}\left\{\tilde{A}_{23}\right\}_{i+1/2} + \frac{\left\{\tilde{C}_{23}\right\}_{i+1/2}}{\Delta s_i} \tag{78}$$

$$\{H_{31}\}_{i,\,i} = \{H_{31}\}_{i,\,i+1} = \frac{1}{2}\left\{\tilde{A}_{31}\right\}_{i+1/2} \tag{79}$$

$$\{H_{32}\}_{i,\,i} = \{H_{32}\}_{i,\,i+1} = \frac{1}{2}\left\{\tilde{A}_{32}\right\}_{i+1/2} \tag{80}$$

$$\{H_{33}\}_{i,\,i} = \frac{1}{2}\left\{\tilde{A}_{33}\right\}_{i+1/2} - \frac{\left\{\tilde{C}_{33}\right\}_{i+1/2}}{\Delta s_i} \tag{81}$$

$$\{H_{33}\}_{i,\,i+1} = \frac{1}{2}\left\{\tilde{A}_{33}\right\}_{i+1/2} + \frac{\left\{\tilde{C}_{33}\right\}_{i+1/2}}{\Delta s_i} \tag{82}$$

To close the system of equations, it is necessary to add three additional relations, corresponding to the boundary conditions and $3 \times (N_i - 1)$ continuity relations at the nodes with inclination angle discontinuity. It can be written:

$$\hat{j}_{g\,k\times N_t} = \hat{j}_{g\,k\times N_t+1} \tag{83}$$

$$\hat{j}_{l\,k\times N_t} = \hat{j}_{l\,k\times N_t+1} \tag{84}$$

$$\hat{P}_{k\times N_t} = \hat{P}_{k\times N_t+1} \tag{85}$$

where $1 \leq k \leq N_i - 1$. Is is important to verify that the number of nodes of each interval N_t could vary. However, in this work we assume that all the intervals are discretized in the N_t nodes.

It is assumed that the gas and liquid mass injections at the bottom of the riser and the separator pressure at the top of the riser are constant. From Section 3.3 and Eq. (24), it results:

$$\hat{j}_{l\,1} = 0 \tag{86}$$

Considering gas injection at the bottom of the riser, Eq. (25):

$$L_e \frac{d\hat{P}_1}{dt} + \tilde{P}_1 \hat{j}_{g\,1} + j_{g0}\,\frac{T_g}{T_0}\,\frac{P_0}{\tilde{P}_1}\hat{P}_1 = 0 \tag{87}$$

And for the top of the riser where the separator pressure is constant:

$$\hat{P}_N = 0 \tag{88}$$

The square matrices $\underline{G}^*$ and $\underline{H}^*$ (dimension $3N \times 3N$ are defined as the matrices $\underline{G}$ and $\underline{H}$ augmented with the boundary conditions, Eq. (86), (87) and (88), resulting:

$$\{H^*\}_{3N-2,\,N+1} = 1 \tag{89}$$

$$\{G^*\}_{3N-1,\,2N+1} = L_e \tag{90}$$

$$\{H^*\}_{3N-1,\,1} = \tilde{P}_1 \tag{91}$$

$$\{H^*\}_{3N-1,\,2N+1} = j_{g0}\,\frac{T_g}{T_0}\,\frac{P_0}{\tilde{P}_1} \tag{92}$$

$$\{H^*\}_{3N,\,3N} = 1 \tag{93}$$

Table 1. Parameters for S-shaped riser (Park and Nydal, 2014).

Definition	Parameter	Value	Unit
Liquid viscosity	μ_l	1×10^{-3}	$kg/(m\,s)$
Gas viscosity	μ_g	1.8×10^{-5}	$kg/(m\,s)$
Liquid density	ρ_l	1000	kg/m^3
Gas constant	R_g	287	$m^2/(s^2\,K)$
Temperature	T_g	293	K
Buffer length	L_e	130.5	m
Pipe diameter	D	5.08×10^{-2}	m
Pipe roughness	ϵ	1.5×10^{-6}	m
Separator pressure	P_s	1.03×10^5	Pa

Table 2. Geometry for S-shaped riser (Park and Nydal, 2014).

Interval	Nodes	Lenght(m)	Inclination (degress)
1	20	2.50	-5.0
2	20	6.05	-4.0
3	20	1.20	-1.8
4	20	0.50	16.0
5	20	0.50	50.0
6	20	4.00	61.8
7	20	0.60	20.8
8	20	2.00	-31.2
9	20	0.50	-12.0
10	20	0.50	24.0
11	20	0.70	64.0
12	20	1.60	77.0
13	20	1.20	90.0
14	20	1.00	0.0

6.2 Eigenvalues spectrum

Considering the augmented system of equations:

$$\underline{G}^* \left\{ \frac{\partial \underline{\hat{v}}}{\partial t} \right\} + \underline{H}^* \left\{ \underline{\hat{v}} \right\} = 0 \tag{94}$$

the following transformation is applied to the system:

$$\left\{ \underline{\hat{v}} \right\} = \left\{ \underline{\hat{r}} \right\} \exp\left(\lambda\, t\right) \tag{95}$$

where λ is an eigenvalue and $\underline{\hat{r}}$ is an eigenvector. From Eq. (94) and (95):

$$\left(\lambda\, \underline{G}^* + \underline{H}^*\right) \left\{ \underline{\hat{r}} \right\} = 0 \tag{96}$$

The transformation in Eq. (95) reduced Eq. (94) to a generalized eigenvalue/vector problem. Equation (96) has no trivial solution only when λ satisfies the characteristic polynomial:

$$\det\left(\lambda\, \underline{G}^* + \underline{H}^*\right) = 0 \tag{97}$$

For the model presented in Section 2,matrix $\underline{G}^*$ is singular, so a number of solutions equal to its rank is expected in Eq. (97). The stability of the stationary state, obtained in Section 4,is given by the behavior of the real part of the eigenvalues of Eq. (96). If the real part of all eigenvalues is negative, the stationary state is stable and if at least one eigenvalues has positive real part, the stationary state is unstable. The neutral stability boundary is then defined as the hyper-surface in the system parameter space where the highest real part of the eigenvalues is zero.

For a set of flow, geometry and simulation parameters, the system of equations corresponding to the stationary state were solved and the matrices $\underline{G}^*$ and $\underline{H}^*$ were assembled. The numerical procedure was implemented using the software MATLAB (Magrab *et al.*, 2005). The subroutine EIG was used to determine the eigenvalue spectrum.

7. RESULTS

The parameters in Table 1 are chosen for a comparison with experimental data of Park and Nydal (2014), corresponding to a S-shaped riser connected to a separator. In this work, it is considered the same geometry for the simulations except for the nodes of discretization, where it was considered $N = 20$ nodes for each interval. The relation of intervals is presented in Table 2.

As result of the stability solver, Fig. 3 shows a comparison between experimental data for severe slugging (stable and unstable points) and the numerical stability boundary obtained from the proposed model through linear stability analysis approach. It can be observed that the model has a good agreement with the experimental data. The numerical stability line can separate both unstable and stable regions in the stability map as the experimental results showed for the S-shaped riser.

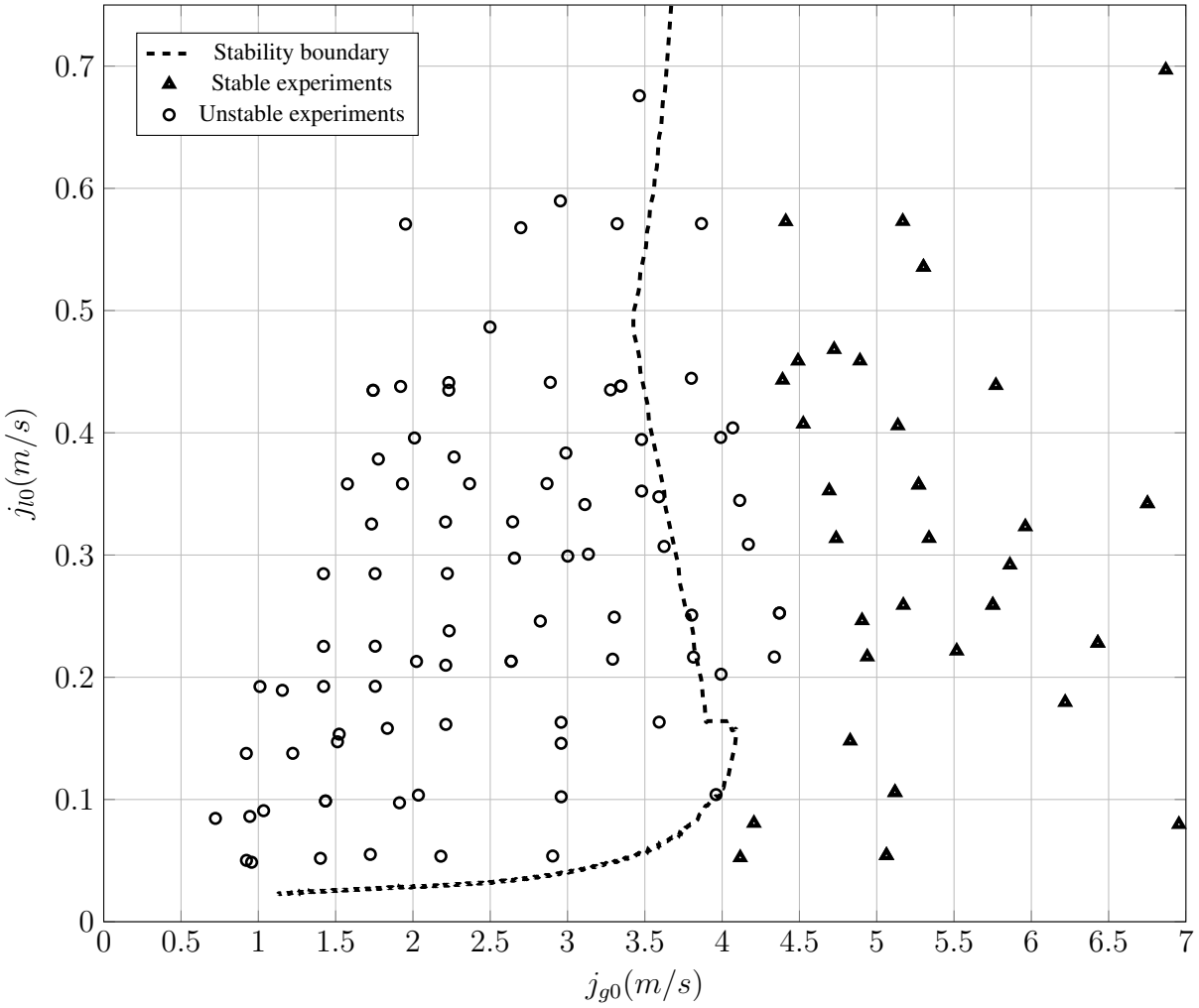

Figure 3. Stability Map - Comparison between numerically stability boundary and experimental data points

8. CONCLUSIONS

In this work was presented a stability solver for air-water hilly terrain flows using stability analysis based on linear stability theory approach. Also, it was considered an general approach to predict the flow pattern and, for each case, to set specific correlations for the two-phase multiplier and the void fraction. The results obtained showed a good agreement with experimental data for S-shaped riser. As discussed in Azevedo *et al.* (2015a), the linear stability theory was proven to be a very efficient tool to predict a map stability for severe slugging.

This model presents a way to predict severe slugging for a S-shaped riser model, however it could be adapted for any air-water hilly terrain flow only by switching the void fraction and friction correlation for others flow patterns. This approach is an general way for any pipeline-riser system to predict severe slugging and it is the main original contribution of this work.

As severe slugging is an important issue in the design of offshore petroleum systems, the necessity of including a stability analysis derived from the dynamic models in computer simulation codes is evident; for the case of stationary simulation codes the necessity is even more important, as the dynamic simulation is not available and the stationary solution may not physically exist.

9. ACKNOWLEDGEMENTS

This work was supported by *Petróleo Brasileiro S. A.* (Petrobras). The authors wish to thank *Conselho Nacional de Desenvolvimento Científico e Tecnológico* (CNPq, Brazil) and *Agência Nacional de Petróleo*, (ANP, Brazil).

10. REFERENCES

Almeida, A.R. and Gonçalves, M.A.L., 1999. "Venturi for severe slug elimination". *Proceedings of 9th International Conference Multiphase*, Vol. American Society of Mechanical Engineers, p. 10.

Azevedo, G.R., Baliño, J.L. and Burr, K.P., 2015a. "Linear stability analysis for severe slugging in air-water systems considering different mitigation mechanisms". *International Journal of Multiphase Flow*, Vol. 73, pp. 238–250.

Azevedo, G.R., Baliño, J.L. and Burr, K.P., 2015b. "Linear stability analysis for severe slugging: sensitivity to void fraction and friction pressure drop correlations". In *Proceeding of the 7th International Conference on Integrated Modeling and Analysis in Applied Control and Automation (IMAACA 2015)*. Bergeggi, Italy, p. 10.

Azevedo, G.R., Baliño, J.L. and Burr, K.P., 2017. "Influence of pipeline modeling in stability analysis for severe slugging". *Chemical Engineering Science*, Vol. 161, pp. 1–13.

Baliño, J.L., 2012. "Modeling and simulation of severe slugging in air-water systems including inertial effects". In *The 6th. International Conference on Integrated Modeling and Analysis in Applied COntrol and Automation (IMAACA 2012)*. Wien, Austria, p. 10.

Baliño, J.L., Burr, K.P. and Nemoto, R.H., 2010. "Modeling and simulation of severe slugging in air-water pipeline-riser systems". *International Journal of Multiphase Flow*, Vol. 36, pp. 643–660.

Bøe, A., 1981. *Severe slugging characteristics. Part I: Flow regime for severe slugging. Part II: Point model simulation study*. Trondheim, Norway.

Chen, N.H., 1979. "An explicit equation for friction factor in pipe". *Ind. Engng. Chem. Fundam.*, Vol. 18, pp. 296–297.

Chexal, B., Lellouche, G., Horrowitz, J. and Healer, J., 1992. "A void fraction correlation for generalized applications". *Progress in nuclear energy*, Vol. 27, No. 4, pp. 255–295.

Jansen, F.E., Shoham, O. and Taitel, Y., 1996. "The elimination of severe slugging - experiments and modeling". *International Journal of Multiphase Flow*, Vol. 22, No. 6, pp. 1055–1072.

Magrab, E.B., Azarm, S., Belachandran, B., Duncan, J.H., Herold, K.H. and Walsh, G.C., 2005. *An Engineer 's Guide to MATLAB*. Pearson Prentice Hall.

Mokhatab, S., 2010. *Severe slugging in offshore production systems*. Nova Science Publishers, Inc., New York.

Müller-Steinhagen, H. and Heck, K., 1986. "A simple friction pressure drop correlation for two-phase flow in pipes". *Chem. Eng. Process.*, Vol. 20, pp. 297–308.

Nemoto, R.H. and Baliño, J.L., 2012. "Modeling and simulation of severe slugging with mass transfer effects". *International Journal of Multiphase Flow*, Vol. 40, pp. 144–157.

Park, S. and Nydal, O.J., 2014. "Study on severe slugging in an s-shaped riser: small-scale experiments compared with simulations". *Oil and Gas Facilities*, pp. 72–80.

Pots, B.F.M., Bromilow, I.G. and Konijn, M.J.W.F., 1987. "Severe slug flow in offshore flowline/riser systems". *SPE Production Engineering*, pp. 319–324.

Sarica, C. and Shoham, O., 1991. "A simplified transient model for pipeline-riser systems". *Chemical Engineering Science*, Vol. 46, No. 9, pp. 2167–2179.

Shoahm, O., 2006. *Mechanistic Modeling of Gas-Liquid Two-Phase Flow in Pipes*. Society of Petroleum Engineers.

Taitel, Y., 1986. "Stability of severe slugging". *International Journal of Multiphase Flow*, Vol. 12, No. 2, pp. 203–217.

Taitel, Y. and Dukler, A.E., 1976. "A model for predicting flow regime transitions in horizontal and near horizontal gas-liquid flow". *AIChE Journal*, Vol. 22, No. 1, pp. 47–55.

Taitel, Y., Vierkand, S., Shoham, O. and Brill, J.P., 1990. "Severe slugging in a riser system: experiments and modeling". *International Journal of Multiphase Flow*, Vol. 16, No. 1, pp. 57–68.

Wordsworth, C., Das, I., Loh, W.L., McNulty, G., Lima, P.C. and Barbuto, F., 1998. *Multiphase Flow Behavior in a Catenary Shaped Riser*. CALtec Report No.: CR 6820, Bedford, UK.

Zakarian, E., 2000. "Analysis of two-phase flow instabilities in pipe-riser systems". In *2000 ASME Pressure Vessel and Piping Conference*. ASME, Seattle, Washington, USA, pp. 1–9.

11. RESPONSIBILITY NOTICE

The authors are the only responsible for the printed material included in this paper.